

Complementary techniques to assess physical properties of a fine soil irrigated with saline water

Angelo Basile · Gabriele Buttafuoco ·
Giacomo Mele · Anna Tedeschi

Received: 15 April 2011 / Accepted: 3 October 2011 / Published online: 21 October 2011
© Springer-Verlag 2011

Abstract Water flow and solute transport numerical modeling is strongly limited due to the lack and difficulty in obtaining hydraulic property data in saline soils. A comparison of different techniques for physical characterization of soil structure is carried out in this study aiming to emphasize the complementarities and the synergy of the different approaches and their suitability for soils affected by salinization. In situ measurements of hydraulic conductivity (HC) by tension disc infiltrometer, water retention (WR) characteristics and pore size distribution by image analysis on undisturbed soil samples and aggregate stability have been measured in lab on a light clay soil of an experimental field undergone to two extreme irrigation treatments, NS (not-saline water, $EC_w = 0.9 \text{ dS m}^{-1}$) and S (saline water with 1% of NaCl; $EC_w = 15 \text{ dS m}^{-1}$). Following, the replicates have been denoted with the under script 1 and 2. The results show: a strong reduction of the index of aggregate stability in water, equals to 37 and 34% for NS_1 and NS_2 , respectively, against the values of 18.9% for S_1 and 18.5% for S_2 , respectively. The water retention curves of the S soils, for all the pressure heads investigated, are above those measured on not-saline soils. The image analysis has showed a larger quantity of pores ($>36 \mu\text{m}$) on the not-saline soils with respect to the saline ones. The total porosity ($>36 \mu\text{m}$) was 21.8% for NS_2 and 11.9% for S_1 . This porosity reduction (9.9%) was spread over the entire ranges of pores with the greatest reduction in pore classes lying in the size range between 700 and 2,000 μm . The unsaturated hydraulic conductivity of the not-salines

samples shows higher values respect to those of the saline samples. All the techniques applied showed converging results and provided a specific contribution towards the demonstration of a process of clogging of macropores under saline condition. Furthermore, the direct measurement of the pore changes provided by soil image analysis allowed a detailed interpretation of the mechanisms behind soil pore-structure worsening due to salinity. Combined use of the tension disc infiltrometer and image analysis methods showed the highest potential to overcome difficulties in hydraulic characterization close to saturation in salinized horizons.

Keywords Aggregate stability · Water retention · Hydraulic conductivity · Image analysis · Pore-size distribution · Salinity

Introduction

Knowledge of soil hydraulic properties is required for predictive purposes and it is crucial in the application of soil water flow and solute transport numerical models. The poor availability of hydraulic property data is, indeed, the main obstacle for applying such models in saline soils (Messing and Jarvis 1993; Šimuněk et al. 1998).

Secondary salinization due to, for example, irrigation with high sodium concentration, may result in the worsening of soil physical properties, through clay particle swelling and dispersion (Feigin et al. 1991) that affects land productivity (Frenkel et al. 1978; Keren and Ben-Hur 2003).

Several researchers have addressed the change in the soil physical properties due to secondary salinization. Among others (Frenkel et al. 1978; Pupisky and Shainberg

A. Basile · G. Buttafuoco · G. Mele · A. Tedeschi (✉)
Institute for Agricultural and Forest Systems in the
Mediterranean (CNR-ISAFOM), National Research Council
(CNR) of Italy, Via Patacca 85, 80056 Ercolano, Naples, Italy
e-mail: Anna.Tedeschi@cnr.it

1979; Shainberg et al. 1981a, b; Shainberg and Letey 1984; Shainberg et al. 1992; Amézketa 1999; Tedeschi et al. 2007) have found a reduction in hydraulic conductivity (HC) following a soil salinity increase. The main mechanisms that have been suggested to explain such a reduction is clay swelling and the dispersion and migration of colloid particles with subsequent clogging of macropores (Rengasamy et al. 1984; Varallyay and Szabolcs 1974; Quirk and Schofield 1955; Rowell et al. 1969). In fact, Jordán et al. (2004) explain that the accumulation of cations such as Na in the soil solution and the exchange phase affect the physical properties of the soil including structural stability, HC, infiltration rate (IR) and soil erosion. In particular, Wang et al. (2008) stress that the most evident changes in land degradation occurred on the surface and near-surface layers of the soil.

Despite the relatively large amount of data on the effect of salt on HC, very little information is available about the effects on the water retention curve (WRC). Dane and Klute (1977) found a decrease in bulk density and an increase in the volumetric water content θ at a pressure head h of -75 cm. This was explained by a reduction in the larger pores with a consequent increase in smaller pores. Somani (1991) found a close relationship between the degree of Na-saturation and the water retention (WR) of the soil, especially in the pressure heads 100–1,000 cm range. Water retention increased over the entire range of soil water content and by contrast, macropore space decreased. However, it should be pointed out that the above considerations about pore changes were derived from indirect measurement of the porous system. Varallyay (1981) studied the effect of various Na-solutions (0.05 N, 0.1 and 0.5 N NaCl and Na₂CO₃) on the WR of two soils: a calcareous loamy and a slightly calcareous clay loam soil. He found a small increase in WR for the lower salt concentrations and larger differences for the 0.5 N treatment especially for the Na₂CO₃ solution. All the effects were more pronounced in the clayed swelling soil. The author explains such a WR increase with the gain in alkaline hydrolysis following the increased exchangeable sodium percentage (ESP).

The aggregate stability can provide lumped information capable to compare the effects of salt concentration as destabilizing factor of the soil structure. The index of aggregate stability in water (IASW) then evaluates such a soil physical property. It becomes greater with increasing clay content (Kemper and Koch 1966; Shainberg et al. 1992) and decreases with increasing salt concentration (Shainberg et al. 2001; Kay and Angers 1999). According to Shainberg et al. (2001) and Kay and Angers (1999) the volume fraction of pores >30 μm and the continuity of these pores mainly determine the (near-saturated) HC of soils. In a soil with stable aggregates, the volume fraction

of the larger pores (>30 μm) is high and so the HC. The same author reports that the disintegration of aggregates into silt-size aggregates (<50 μm) results in a decrease of HC of the soil. Also Levy et al. (2005) report that aggregates slaking and subsequent change in pore size distribution (PoSD) may reduce the hydraulic conductivity, infiltration rate and lead to runoff and erosion.

All the changes of the physical properties due to salinization basically derive from the change in the soil structure and, specifically, in a re-arrangement of the porous space. In this respect, image analysis of the pore network was recently applied to compare the effects of different irrigation treatments on pore size geometry (Tedeschi et al. 2002). Moreover, it can be applied to compare pore-size distributions derived from the WRC (Basile et al. 2007), to infer effective hydraulic properties (Vogel and Roth 1998, 2001), and linking tortuosity parameters (Vervoort and Cattle 2003) to pore space geometry and pore-size distribution.

Finally, measuring hydraulic properties in saline soils with standard methods is difficult but this can be partially overcome using tension disc infiltrometer method (Angulo-Jaramillo et al. 2000). It is being widely used for in situ measurement of unsaturated soil hydraulic conductivity at water pressure heads near saturation and also to detect changes in porous space (Ankeny et al. 1991; Perroux and White 1988; Angulo-Jaramillo et al. 2000). The tension disc infiltrometer method should theoretically also be applicable in saline soil, where other methods can fail, but rare applications have been found in the literature (Mennee et al. 2001; Ghiberto et al. 2007).

Literature reviewed above generally addresses the dependence of a single soil physical property on soil salinity, while no study provided evidences from concurrent measurements of multiple soil physical properties under saline and non-saline conditions. Only a preliminary study (Huang et al. 2010) reports the application of some different techniques applied on saline and non-saline soils to attempt, on part, the observation of changes in soil physical characteristics.

Summarizing, the application of saline water was associated with: (1) reduction of connectivity of the pore space because of dispersion and migration of colloids particles with subsequent clogging of macropores and reduction in HC; (2) larger fraction of pore space represented by smaller pores, due to the re-arrangement of clay particles, with subsequent modification of the WRC; (3) lower cohesion of soil aggregates due to the dispersion effects operated by the salt presence.

Our hypothesis and research question is whether such processes are observable by measuring specific soil physical properties and their level of interaction. Specifically, (1) unsaturated HC and PoSD to establish whether a

modification in the fraction of pore space accounted by large pores does occur and over which pore size range; (2) WRC to establish whether an increase of pore space at smaller pore size does occur and over which pore size range; (3) IASW to establish the cohesion of soil particles does occur.

In addition to the better understanding of the soil physical processes induced by saline water irrigation, the aim of this study is, therefore, to address the research question above by evaluating whether such changes do indeed occur simultaneously and to assess whether all observed changes were consistent with each other. For this purpose the comparison of the results between the different techniques applied refers, whenever possible, to measurements performed on the same soil sample.

Materials and methods

Experimental site

The study was performed at the CNR-ISAFOM experimental farm (43 ha) located in the Volturno river plain at 25 m a.s.l., 14°12' long. E and 41°07'N [Vitulazio (CE), southern Italy]. Mean annual precipitation is 584 mm distributed over 81 rainy days, and mean annual air temperature is 17.2°C. Alluvial processes formed the sedimentary soils of the farm and the soil where the experiment was performed was classified as Vertic Haplustept (Soil Survey Staff 2010). Moreover, the texture of the soil is light clay according to the International Union of Soil Science (IUSS) (see Table 1). The main chemical characteristics of the top layer were the following: CEC 27.5 cmol(+) kg⁻¹; Ca 25.3 cmol(+) kg⁻¹; Mg 1.4 cmol(+) kg⁻¹; K 0.5 cmol(+) kg⁻¹; Na 0.3 cmol(+) kg⁻¹; total carbonate 2.9%.

From 1995 till 2001 in an area of about 1 ha, belonging to the experimental farm, a randomized experiment, with four replications to evaluate the effects that three levels of

saline water had on crop production and on the soil chemical–physical characteristics, was designed (d’Andria et al. 1997; Tedeschi and Dell’Aquila 2005). The levels of salinity tested were: a treatment irrigated by well water, not-saline and three treatments obtained by adding to the not-saline water 0.25, 0.5 and 1% of NaCl. The experimental set-up was the same throughout the 7 years and the saline treatments were repeated each year on the same plots. Each plot had a size of about 150 m².

At the end of the experimental trials (September 2001), until May 2002, the soil was under rainfall condition and over this time about 408 mm occurred. Table 1 reports the main soil characteristics of the layer 0.0–0.2 m, for the saline (S) and not saline treatments (NS) where the measurements were carried out.

Field measurements and sampling

Measurements and sampling were performed in June 2002 on the plots subjected to the two extreme treatments: the NS irrigated by not saline water (EC_w = 0.9 dS m⁻¹) and the S irrigated with water added with 1% of NaCl (EC_w = 15 dS m⁻¹). Following, the replicates have been denoted with the under script 1 and 2.

Infiltration measurements were performed in duplicate, on both sites of NS and S, by tension disc infiltrometer (Ankeny et al. 1991) for near-saturation hydraulic conductivity determination. The apparatus has a 20-cm diameter disc with a highly permeable nylon membrane to be placed in contact with the soil. The instrument has also a tower-reservoir of water for measuring infiltrating water and a Mariotte’s bottle system imposing the pressure head. Cumulative infiltration *I(t)* was recorded until the steady-state infiltration rate was reached at five soil water pressure heads: -12, -9, -6, -3, and -1 cm.

Hydraulic conductivity was estimated from Wooding’s solution (1968) for steady-state flow from a shallow

Table 1 Soil characteristics for the layer 0.0–0.2 m of the soils, classified as light clay according to International Union of Soil Science (IUSS), where the measurements were carried out

Treatments	Sand (g kg ⁻¹)	Silt (g kg ⁻¹)	Clay (g kg ⁻¹)	pH (-)	OM (%)	ECe ^a (dS m ⁻¹)	ESP (%)
NS ₁	305.0 (38)	378.3 (49)	316.7 (32)	7.2 (0.01)	1.7 (0.08)	0.95 (0.09)	1.6 (0.40)
NS ₂	391.7 (2.9)	263.3 (2.9)	345.0 (5)	7.1 (0.03)	2.1 (0.15)	0.81 (0.06)	1.2 (0.30)
S ₁	368.0 (16)	286.0 (13)	326.0 (2.9)	7.2 (0.03)	1.6 (0.11)	5.00 (0.75)	19.0 (1.14)
S ₂	363.3 (37)	291.7 (36)	345.0 (5)	7.2 (0.02)	1.4 (0.08)	4.20 (0.35)	16.0 (1.35)

NS is the not saline soil and S is the saline soil; the subscription, 1 and 2 indicates the replicate. The pH, organic matter (OM), electrical conductivity of the saturated paste (ECe) and percentage of the exchangeable sodium (ESP) are reported. In table the standard deviation is reported between brackets in italic for each parameters

^a EC_e of the saturated paste was determined according to Rhoades (1996)

circular pond. It assumes that flow is described by Darcy's equation and that soil is uniform with initial water potential h_n and volumetric water content θ_n . The soil is dry initially with h_n tending to $-\infty$ and hydraulic conductivity $K(h_0)$ is given by the quasi-linear Gardner model (Gardner 1958):

$$K(h_0) = K_{fs} \exp(\alpha h_0) \quad (1)$$

where $K(h_0)$ is the unsaturated conductivity at a given pressure head h_0 , K_{fs} is the field-saturated hydraulic conductivity and α is the exponential slope. Analysis of tension disc infiltrometer data was made following the multiple head approach that requires two or more steady-state flow values for a single disc radius at different pressure heads to obtain a piecewise relationship $K(h_0)$ (Coppola et al. 2009). Finally, assuming the slope of the curve to be constant from the last measured value and the saturated hydraulic conductivity, K_s is calculated from Eq. 1 (Jarvis and Messing 1995). Details about the technique can be found in the review of Angulo-Jaramillo et al. (2000).

At the end of the measurement and exactly below the position where the disc of the tensiometer was placed, undisturbed soil samples were collected in aluminium cylinders (600 cm³; height 12 cm and \varnothing 8 cm) for measuring the pore-size distribution by image analysis and in steel cylinders of about 600 cm³ (height 12 cm and \varnothing 8 cm) and 270 cm³ (height 7 cm and \varnothing 7 cm) for water retention and bulk density measurements. Moreover, bulk soil was collected for texture and aggregate stability analysis.

Laboratory analysis

Texture and IASW

The texture was determined by the pipette method after the removal of soluble salts and organic matter (Gee and Bauder 1986). The aggregate stability in water was measured by an apparatus at vertical oscillation developed at the ISAFOM (Dell'Aquila 2007). For both determinations the analysis was performed on three replicates for each treatments. On bulk soil collected at 0.0–0.2 m depth the aggregate stability measurements were performed on 10 g of soil aggregates which had a diameter in the 1–2 mm range. Aggregates were non-wetted and shaken at a speed of 30 cycles per minute with a sieve stroke length of 3 cm. The index of aggregate stability, IASW, defined by the following equation:

$$IASW = 100 * \left(1 - \frac{W_4}{W_{48}} \right) \quad (2)$$

was calculated from the weight of the aggregates dispersed in water after shaking for 4 (W_4) and 48 (W_{48}) minutes.

Water retention curve

The undisturbed soil samples were slowly saturated from the bottom in the laboratory. Three tensiometers were installed at three different depths in the NS samples of about 600 cm³ and placed on a load cell; starting from saturation and during a 1-dimensional transient upward flow, the pressure head and weight of the sample were automatically recorded at these depths until air was observed in the circuit of the uppermost tensiometer. After that, the soil sample was dismantled and placed for 24 h in the oven at 105°C to determine the water content from the weight data set (Basile et al. 2006).

An iterative method was applied to obtain the WRC (Tamari et al. 1993; Coppola et al. 2009). We used the well-known van Genuchten (1980) relationship:

$$S_e(h) = \frac{\theta(h) - \theta_r}{\theta_s - \theta_r} = (1 + |\alpha h|^n)^{-m} \quad (3)$$

where $S_e[-]$ is the effective fluid saturation, $\theta(L^3 L^{-3})$ is the volumetric water content with θ_r and θ_s being the residual and the saturated water content, respectively. We started with a guessed WRC, obtained by an initial estimate of fitting parameters of van Genuchten relationship to convert pressure head data at anyone time into estimated water contents at the tensiometer depths. Average water content of the soil sample was then calculated and compared with the average measured water content obtained from the sample weight. If significant differences between calculated and measured average water content were observed, a new parameter set was estimated. The WRC was optimized using an iterative procedure, by minimizing the squared differences between calculated and measured average water content. After convergence of the algorithm, water contents at the tensiometer depths were calculated from the measured pressure heads and the estimated WRC.

On the smaller sample of about 200 cm³, the soil WRC $\theta(h)$ was determined for the S soil samples by means of the tension table (Dane and Hopmans 2002). Nine points of the curve ranging between near saturation and -300 cm of potential were measured.

Pore size distribution by soil image analysis

Undisturbed cylindrical samples of soil were impregnated with fluorescent resin via saturation from the bottom. After resin hardening, square cuboid shaped soil blocks were cut from each one and the four vertical rectangular faces were polished and then lit with UV (365 nm) lamps (Mele et al. 2000). Then digital images of eight vertical sections (width 4.7 cm, depth 7.2 cm) for each treatment at a pixel resolution of 18 μ m were acquired using a Nikon D200 digital SLR camera. Images were binarised by simple threshold

method using Corel X3 software (<http://www.adobe.com>) and used to perform image analysis of the pores. In Fig. 1 on the left side is shown the block after the UV lamps treatment and on the right side the sequence of the four vertical sections after binarisation.

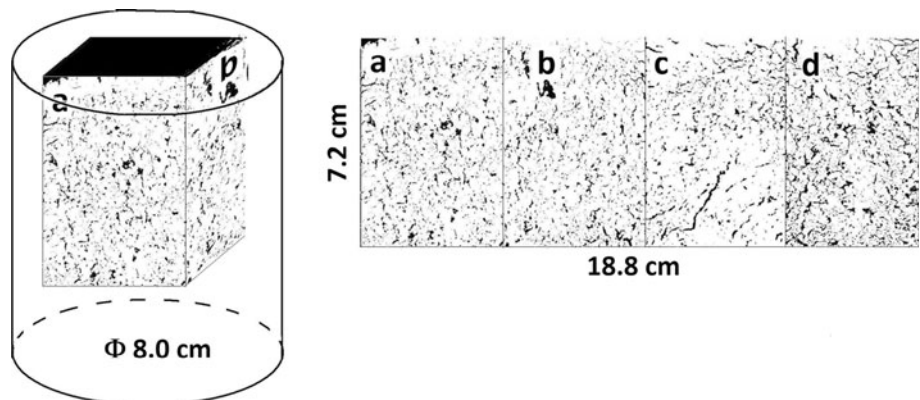
The pore-size distribution analysis was based on the ‘opening’ algorithm of mathematical morphology (Serra 1982; Horgan 1998) using a code written in C language developed by Moreau (1997) and updated by Mele et al. (1999). The software works by applying successively, on the pixels representing the porous phase, the operator of ‘opening’ with a sphere (circle in 2D) of increasing radius as ‘structuring element’. The resulting effect is that of a series of virtual spheres with an increasing diameter which run throughout the entire pore network and fill voids with space between opposite walls smaller than or equal to the current diameter. At each increase in diameter the difference between the initial porosity and the residual one, resulting after filling the pores with the current sphere (circle), is calculated. The overall result is the partition of the pore space according to the wall distance. In Fig. 2 on the left-side is shown an example of a small part of soils where different colours correspond to different diameters of the virtual circle. On the right side the corresponding frequency histogram of pore-size classes is also shown.

The image analysis techniques that we used allowed correct discrimination of only the pores with a size at least twice the image resolution (18 μm in this case). Therefore, the porosity values reported here do not refer to the pores smaller than 36 μm.

Results and discussion

In Table 1 texture and main chemical characteristics of the four investigated soil samples are reported. Following, we first show the separate results for each applied technique and then the comparison among samples and techniques.

Fig. 1 Example on the not-saline (NS) soil sample of square cuboid shaped soil block cut from undisturbed sample impregnated with fluorescent resin then lit with UV lamps and binary image of the four vertical sections put side by side



Prior to go in the discussion we have to recall that the objective of this study was to address whether observed changes in physical properties were consistent each other, trying to emphasize the complementarities and the synergies of the different approaches applied. In this sense, the comparison was made on each site (soil sample) of measurement, for all the four applied techniques:

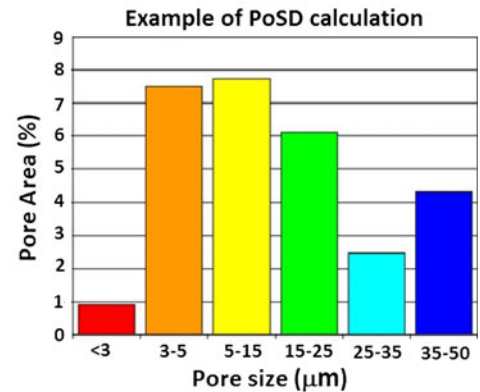
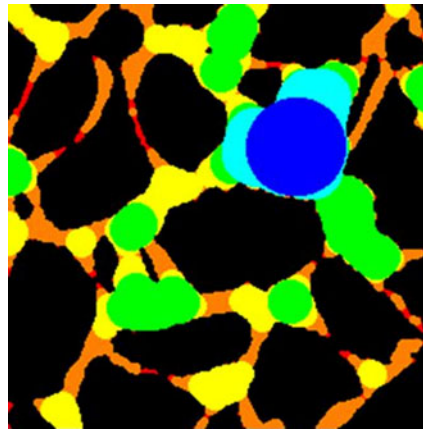
Structure stability

Irrigation with saline water produced a well-known effect on the soil structure stability. In fact, although the four soil samples showed similar texture, organic matter and pH, the soil stability index, IASW, decreased markedly from NS ($37 \pm 3\%$ SD for NS₁ and $34 \pm 3\%$ SD for NS₂) to S (18.9 ± 0.7 SD for S₁ and $18.5\% \pm 0.8$ SD for S₂) treatments. Huang et al. (2010) reported similar results for soils of the NW of China having a higher sand fraction. This reduction in structure stability expressed by the IASW was related to the increasing of ESP values as reported in Table 1. The high levels of ESP for the S treatments, due to the presence of Na, contribute to increase the clay dispersion that causes the clogging of pores (Shainberg and Letey 1984; Quirk and Schofield 1955) with a direct effect on soil structure. These results show that the addition of NaCl on the soil under study reaches in clay (about 33%) strongly contribute to the degradation of the soil structure. This effect can result in unfavourable agronomic conditions (e.g., higher risk of water ponding, formation of superficial crusts that may affect plant emergence). Hence, although the aggregate stability technique does not offer a simple and univocal physical meaning, it clearly indicates the salt concentration as destabilizing factors of the soil structure.

Water retention

Figure 3 shows the experimental $\theta(h)$ points for NS and S soil samples. The WRCs of the S soils, for all the pressure heads investigated, are above those measured on soils

Fig. 2 Exemplification of pore size distribution (PoSD) by “successive opening” procedure. Pore space is partitioned according to the minimum distance between opposite walls of the solid phase



irrigated with not-saline water. This finding is in accord to the results found by few researchers (i.e., Dane and Klute 1977; Varallyay 1981), showing higher retention values in soil with higher salt content following a primary or secondary salinization. The WRCs of samples NS₁ and NS₂ are similar in the drier range while they deviate for pressure heads higher than -45 cm, resulting in larger water content close to saturation (about 6%) for NS₂. This result is in agreement with the higher organic matter contents (Table 1) shown by NS₂ versus NS₁. On the contrary, S₁ and S₂ samples do not show relevant differences for all the investigated range of pressure heads.

Pore-size distribution

In Fig. 4 are shown examples of binary images of two sections from NS and S treatment, respectively, where

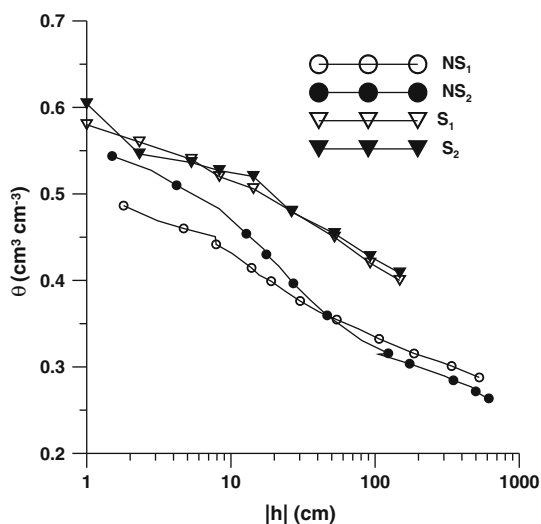


Fig. 3 Water retention curve measured on surface soil horizon on soil irrigated with not-saline (NS₁ and NS₂) and saline water (S₁ and S₂)

pores are in black. What immediately comes up from a visual inspection of the two images is the larger size of the pores (>36 μm) showed by the NS (left) image respects to the S one (right). With image analysis, we directly measured the pore-size distribution. Results refer to four images for each soil sample. Figure 5 shows, in the lower part of the graph, the pore-size distributions of the NS (grey) and S (black) treatments. Moreover, in the upper part of the graph are the relative percent differences (RPDs) between the two treatments being:

$$RPD = \frac{P_s(i) - P_{NS}(i)}{\max[P_s(i); P_{NS}(i)]} \quad (4)$$

where i is the i th pore size class and $P_{NS}(i)$ and $P_S(i)$ are the porosity values at i th pore size class for NS₂ and S₁ samples, respectively. Each class of pores have an increment of 36 μm, which is also the lower detection limit due to the resolution of the technique.

The results of the samples NS₂ and S₁ have been purposely compared in Fig. 5 for their similar texture and organic matter content, which more reliably allowed correlating the differences due to the saline treatment.

Total porosity (>36 μm) was 21.8% for NS₂ and 11.9% for S₁. This porosity reduction (9.9%) was spread over the entire ranges of pores with the greatest reduction in pore classes lying in the size range between 700 and 2,000 μm. More precisely, according to the RPD index, it can be observed that the percent reduction of pores increases with pore size and there is an almost complete disappearance of the pores larger than approximately 2,000 μm (about -100% of the RPD index). It is worth noting that the general clogging of those large pores produced, however, new pores having size of about 2,500 and 3,200 μm. This seems to confirm the hypothesis stated by Dane and Klute (1977) on the soil pore redistribution following saline treatment. Moreover, similar results were found by Tedeschi et al. (2007) for soils with abundance of smectite-type clay minerals.

Fig. 4 Examples of binary images of vertical soil sections from not saline (NS) and saline (S) treatments

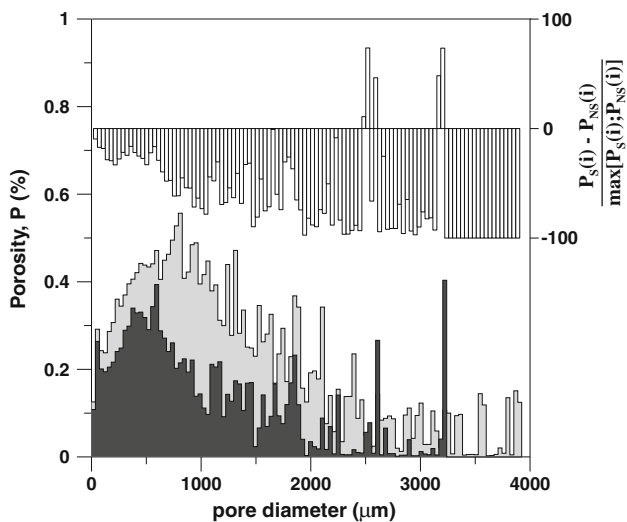
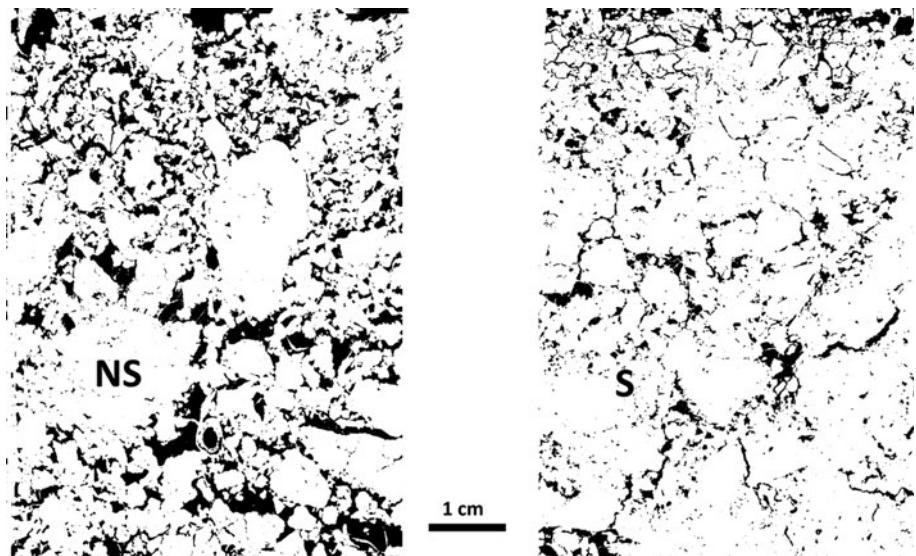


Fig. 5 Pore size distributions measured by image analysis for not-saline (NS grey) and saline (S black) treatment. The relative percent differences (RPDs) between the two treatments have been reported on the right-hand axis

The limits in the detectable size-range of pores analyzed by image analysis, due to the threshold of the image resolution, can be overcome by deriving the equivalent pore-size distribution from the soil WRC. Assuming that the porous system can be simply described as a bundle of parallel capillaries and replacing the soil water pressure head by the pore-diameter according to the bi-univocal capillarity equation ($|h| \approx 0.3/d$, for length unit in cm), the WRC can be seen as a cumulative distribution function of ‘equivalent pore-size’ (Brutsaert 1966). The resulting equivalent diameters are those of the bundle of capillary tubes that behave, in functional terms, as the soil sample. The procedures adopted are those reported by Durner

(1994), fitting the experimental data by the five-parameters function of van Genuchten (1980).

The results are shown in Fig. 6 where the vertical line represents the lower limit of the image analysis measurement. It can be noticed that below such pore size limit, the S treatment has overall produced an increase of pores not detectable using image analysis only to quantify changes in pore structure. A crossover point between both the S curves and that of the NS₂ sample was detected at around 20–30 μm. However, although the two approaches of pore space quantification are quite different, they overall agree for pores larger than 36 μm and no crossover point between NS₂ and S (Figs 5, 6) was evident.

Then, measurements of pore-size distribution by water retention can be used—in the pressure head range where

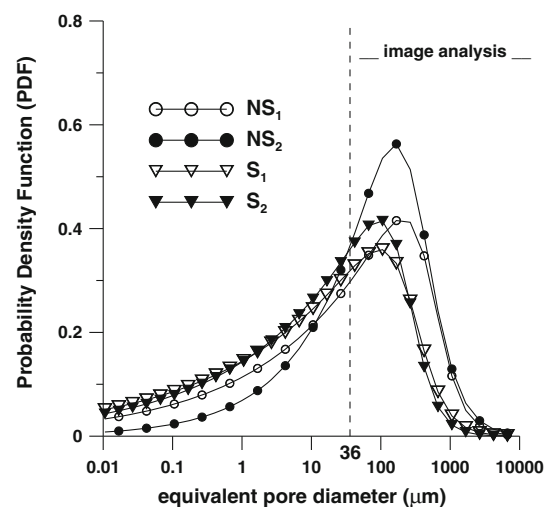


Fig. 6 Equivalent pore-size distributions derived from water retention curves on the surface soil horizon of the not-saline (NS) and saline (S) soil samples

the capillarity law still apply—to investigate the pore-size range below the digital image pixel resolution where no direct measurements by image analysis can be available.

Hydraulic conductivity

Figure 7 shows the unsaturated hydraulic conductivity curves measured by the tension disc infiltrometer. The NS curves respect to the S curves show higher values of hydraulic conductivity for each measured value of pressure head. S_1 and S_2 samples do not show relevant differences for all the investigated range of pressure heads while NS_1 and NS_2 samples show remarkable differences close to the saturation only. Finally, all the curves show similar slope except than that of the sample close to the saturation.

To clarify such a discrepancy between the two NS samples, the comparison between unsaturated hydraulic conductivity and PoSD of the two not-saline soil samples (NS_1 and NS_2) was also performed. Equivalent pore diameters were calculated from the pressure head in the range where hydraulic conductivity was actually measured. This allowed plotting both the PoSDs (Fig. 8) determined from image analysis and the hydraulic conductivity as a function of pore diameter.

In Fig. 8 the unsaturated hydraulic conductivity curves (right axis) and the absolute porosity (left axis) of the two NS treatments are reported versus pore-diameters. The two $K[h(d)]$ curves show a crossover point between the measuring points at 380 and 620 μm with an estimated average of about 500 μm . Porosity analysis showed that the crossover point, where the frequency of pores became higher in soil NS_2 than in soil NS_1 , is located between 540

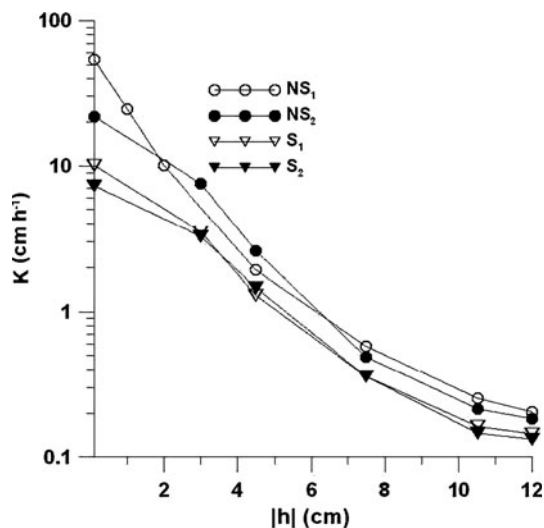


Fig. 7 Unsaturated hydraulic conductivity measured on surface soil horizon by tension disc infiltrometer on soil irrigated with not-saline water (circles NS_1 and NS_2) and with saline water (triangles S_1 and S_2)

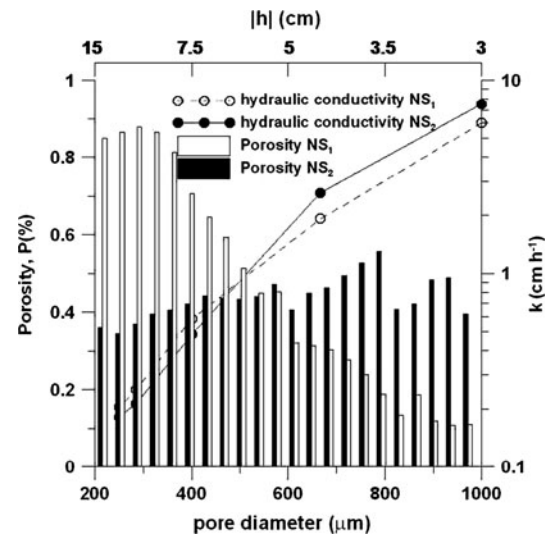


Fig. 8 Unsaturated hydraulic conductivity (right axis) versus pore diameter for the not-saline treatments (NS) for the soil sample NS_1 (circles) and NS_2 (filled circles). Pore-size distributions (left axis) of treatment NS_1 (white) and NS_2 (black)

and 576 μm . Hence, in the above range of h the pore-size distributions measured by image analysis, validated the accuracy of the $K(h)$ curves measured by tension disc infiltrometer and the related information fully converge.

Finally, as last example of convergence between methodologies, Fig. 9 shows a comparison between $K(h)$ curve and PoSD for NS and S treatments (employing the same soil samples used for Fig. 5) in the range of h (or corresponding pore diameter d) where hydraulic conductivity

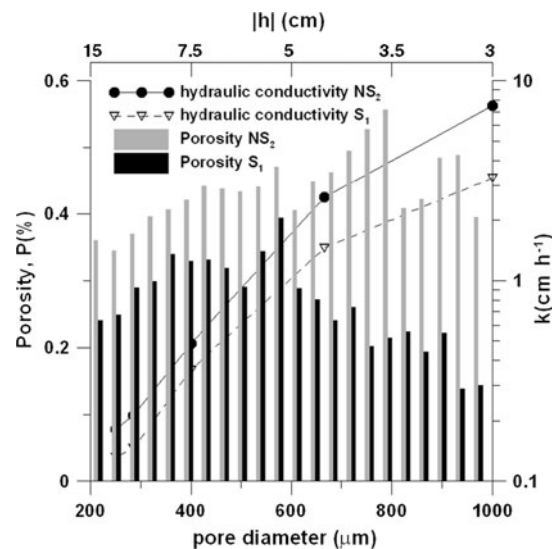


Fig. 9 Unsaturated hydraulic conductivity (right axis) versus pore diameter assuming $|h| \approx 0.3d$. Pore-size distribution of the not-saline sample NS_2 (grey) and the saline sample S_1 (black) for the same pore range of the hydraulic conductivity data is reported (left axis)

was actually measured. The agreement between the methodologies is confirmed by the similar trends, at increasing d , of the differences in unsaturated hydraulic conductivity between the not-saline (NS_2) and saline (S_1) soil samples and the differences in porosity towards large pore-diameters (to note that the hydraulic conductivity values on the right-hand axes are on log-scale). This result is in accord with the Hagen–Poiseuille equation stating that the mean flow rate in a capillary is a square function of the pore radius; therefore, larger pores mainly contribute to the flux density and hydraulic conductivity (Kutilek and Nielsen 1994).

Conclusion

Most of scientific literature provides examples of observations of changes in a single soil property under saline and not-saline conditions. Concurrent measurements of multiple soil physical properties under saline and not-saline manipulations are rarely reported.

The results have shown that all the measured properties, independently from the applied technique, have clearly pointed out a change of the soil physical conditions due to irrigation with saline water. Halving of the soil stability index IASW, reduction in near-saturated hydraulic conductivity and porosity reduction in the whole pore-size range investigated by image analysis are evidences of soil structure deterioration. In the range of small pore size an increase in water retention was also detected. More specifically, results have pointed out:

1. a clogging of macropores under saline condition. Swelling and dispersion of clay determine the migration of colloid particles and subsequent macropore clogging as reported by several authors. The macropores reduction observed in this case study when comparing not-saline with saline soil samples is consistent for all the four variables used to analyze it. Indeed: (1) a strong reduction of the soil stability index IASW, (2) an increase in water retention and consequent shifting of the equivalent pore-size distribution towards smaller pores, (3) a reduction in near-saturated hydraulic conductivity and (4) a porosity reduction in the whole pore-size range investigated were observed.
2. the suitability of pore image analysis for direct measurement of the pore changes. This affording better interpretation of the mechanisms behind soil pore-structure worsening due to salinity, which are generally explained by indirect measurements often based on mere undemonstrated assumptions. Then, the pore-size distribution analysis in the range below the image resolution can be extended through the indirect estimation obtained by water retention.
3. an excellent convergence, in both saline and not-saline soil samples, in determining physical properties based on completely different approaches. For example, in the case of the two not-saline soils the measured crossover point of the two hydraulic conductivity curves matches those estimated from the image analysis. This consistency between the two measurements suggests the potentiality of the tension infiltrometer and image analysis methods to overcome difficulty in obtaining hydraulic property data for physically based model application. Specifically, the tension disc infiltrometer technique can be an effective method to characterize near-saturated hydraulic conductivity also in saline clayed soil, where some largely applied techniques can fail. The occurrence of water flow due to the presence of salt gradients is largely ignored in the application of several methods like the Wind method (Arya 2002) and the inverse method (Hopmans et al. 2002). Furthermore, also the widely applied estimation of hydraulic properties with pedo-transfer functions is hampered by the modification of the soil structure induced by the use of saline water. Moreover, the pore-size distributions obtained by image analysis can be a reliable method to determine unsaturated hydraulic conductivity, especially in soils with some physical (i.e., reduced thickness of the soil horizon) or chemical (i.e., saline soil) limitation. In fact, due to the difficult of hydraulic conductivity measurements, models predicting the $K(h)$ relationship from the equivalent pore-size distribution inferred from the water retention function (i.e., Burdine 1953; Mualem 1976) are widely applied. In this respect, pore size measurements, especially when using techniques with very high spatial resolution (i.e. X-ray microtomography) can be in some cases a valid alternative to the standard technique of $K(h)$ measurement.

Acknowledgment The authors would like to thank Mr. B. Di Matteo for preparing samples for soil image analysis measurements.

References

- Amézketa E (1999) Soil aggregate stability: a review. *J Sustain Agric* 14:83–151
- Angulo-Jaramillo R, Vandervaere JP, Roulier S, Thony JL, Gaudet JP, Vaucelin M (2000) Field measurement of soil surface hydraulic properties by disc and ring infiltrometers: a review and recent developments. *Soil Tillage Res* 55:1–29
- Ankeny MD, Ahmed M, Kaspar TC, Horton R (1991) Simple field method for determining unsaturated hydraulic conductivity. *Soil Sci Soc Am J* 55:467–470
- Arya LM (2002) Wind and hot-air methods. In: Dane JK, Topp GC (eds) *Methods of soil analysis: Part 4-Physical methods*. SSSA Book Series 5. SSSA, Madison, pp 916–926

- Basile A, Coppola A, De Mascellis R, Randazzo L (2006) Scaling approach to deduce field unsaturated hydraulic properties and behavior from laboratory measurements on small cores. *Vadose Zone J* 5:1005–1016
- Basile A, Coppola A, De Mascellis R, Mele G, Terribile F (2007) A comparative analysis of the pore system in volcanic soils by means of water-retention measurements and image analysis. In: Arnalds O et al (eds) *Soils of volcanic regions in Europe*. Springer, Berlin, pp 493–513
- Brutsaert W (1966) Probability laws for pore-size distribution. *Soil Sci* 101:85–92
- Burdine NT (1953) Relative permeability calculations from pore size distribution data. *Trans AIME* 198:71–77
- Coppola A, Basile A, Comegna A, Lamaddalena N (2009) Monte Carlo analysis of field water flow comparing uni- and bimodal effective hydraulic parameters for structured soil. *J Contam Hydrol* 104:153–165
- d'Andria R, De Lorenzi F, Martorella A, Calandrelli D, Tedeschi P, Lavini A, Alvino A (1997) Growth analysis of a field-grown sunflower [*Helianthus annuus* L.] under different salt concentration of irrigation water. In: *Acts of international conference on water management, salinity and pollution control towards sustainable irrigation in the Mediterranean region*, MAI, Bari (Italy), September 22–26, pp 381–394
- Dane JH, Hopmans JW (2002) Water retention and storage. In: Dane JK, Topp GC (eds) *Methods of soil analysis: Part 4-Physical methods*. SSSA Book Series 5. SSSA, Madison, WI, USA, pp 671–720
- Dane JH, Klute A (1977) Salt effects on the hydraulic conductivity of a swelling soil. *Soil Sci Soc Am J* 41:1043–1049
- Dell'Aquila R (2007) Automatic sieve-shaker for determining soil aggregate stability and dimensional distribution using a vertical oscillation system. *Ital J Agron* 4:401–406
- Durner W (1994) Hydraulic conductivity estimation for soils with heterogeneous pore structure. *Water Resour Res* 30:211–223
- Feigin A, Ravina I, Shalhevet J (1991) Irrigation with treated sewage effluent. *Management for environmental protection. Advanced series in agricultural sciences* 17. Springer, Berlin
- Frenkel H, Goertzen JO, Rhoades JD (1978) Effects of clay type and content exchangeable sodium percentage, and electrolyte concentration on clay dispersion and soil hydraulic conductivity. *Soil Sci Soc Am J* 42:32–39
- Gardner WR (1958) Some steady state solutions to the unsaturated flow equation with application to evaporation from a water table. *Soil Sci* 85:228–232
- Gee GW, Bauder JW (1986) Particle-size analysis. In: Klute A et al. (eds) *Methods of soil analysis. Part 1. Physical and mineralogical methods*, 2nd edn. American Society of Agronomy and Soil Science Society of America, Madison, pp 383–411
- Ghiberto PJ, Pilatti MA, Imhoff S, de Orellana JA (2007) Hydraulic conductivity of Molisolls irrigated with sodic-bicarbonated waters in Santa Fe (Argentina). *Agric Water Manag* 88:192–200
- Hopmans JW, Simunek J, Romano N, Durner W (2002) Simultaneous determination of water transmission and retention properties. Inverse methods. In: Dane JH, Topp GC (eds) *Methods of soil analysis. Part 4. Physical methods*. Soil Science Society of America Book Series No. 5, pp 963–1008
- Horgan GW (1998) Mathematical morphology for analysing soil structure from images. *Eur J Soil Sci* 49:161–173
- Huang CH, Xue X, Wang T, De Mascellis R, Mele G, You QG, Peng F, Tedeschi A (2010) Effects of saline water irrigation on soil properties in northwest of China. *Environ Earth Sci*. doi: 10.1007/s12665-010-0738-5
- Jarvis NJ, Messing I (1995) Near-saturated hydraulic conductivity in soils of contrasting texture measured by tension infiltrometers. *Soil Sci Soc Am J* 59:27–34
- Jordán MM, Navarro-Pedreño J, García-Sánchez E, Mateu J, Juan P (2004) Spatial dynamics of soil salinity under arid and semi-arid conditions: geological and environmental implications. *Environ Geol* 45:448–456
- Kay BP, Angers DA (1999) Soil structure. In: Sumner ME (ed) *Handbook of soil science*. CRC Press, New York, pp A-229–A-269
- Kemper WD, Koch EJ (1966) Aggregate stability of soils from western USA and Canada. USDA Technical Bulletin No. 1355. US Government Printing Office, Washington, DC
- Keren R, Ben-Hur M (2003) Interaction effects of clay swelling and dispersion, and CaCO₃ content on saturated hydraulic conductivity. *Aust J Soil Res* 41(5):979–989
- Kutilek M, Nielsen DR (1994) *Soil hydrology*. Catena. Verlag, Geoscience Publ., Amsterdam
- Levy GJ, Goldstein D, Mamedov AI (2005) Saturated hydraulic conductivity of semiarid soils: combined effects of salinity, sodicity, and rate of wetting. *Soil Sci Soc Am J* 69:653–662
- Mele G, Basile A, Leone AP, Moreau E, Terribile F, Velde (1999) The study of soil structure by coupling serial sections and 3D image analysis. In: Feyen J, Wiyono K (eds) *Modelling of transport processes in soils*. Proceeding of international workshop of EurAgEng's field of interest on soil and water. Wageningen Pers, The Netherlands, pp 103–117
- Mele G, Terribile F, Morerau E (2000) Soil structure characterization of selected European volcanic soils. *Agric Med* 130:247–256
- Mennee JC, McLay CDA, Lee R (2001) Effects of sodium contaminated wastewater on soil permeability of two New Zealand soils. *Aust J Soil Res* 39:877–891
- Messing I, Jarvis NJ (1993) Temporal variation in the hydraulic conductivity of a tilled clay soil as measured by tension infiltrometers. *Eur J Soil Sci* 44:11–24
- Moreau E (1997) *Étude de la morphologie et de la topologie 2D et 3D d'un sol argileux par analyse d'images*. Ph.D. Thesis. Université de Poitiers, France
- Mualem Y (1976) A new model predicting the hydraulic conductivity of unsaturated porous media. *Water Resour Res* 12:513–522
- Perroux KM, White I (1988) Designs for disc permeameters. *Soil Sci Soc Am J* 52:1205–1215
- Pupisky H, Shainberg I (1979) Salt effects on the hydraulic conductivity of a sandy soil. *Soil Sci Soc Am J* 43:429–433
- Quirk JP, Schofield PK (1955) The effect of electrolyte concentration on soil permeability. *Soil Sci* 6:163–178
- Rengasamy P, Green RSB, Ford GW (1984) The role of clay fraction in the particle arrangement and stability of soil aggregates—a review. *Clay Res* 3:53–67
- Rhoades JD (1996) Salinity: electrical conductivity and total dissolved solids. In: Spark DL (ed) *Methods of soil analysis. Part 3. Chemical methods*. Soil Science Society of America Book Series No. 5, pp 417–435
- Rowell DL, Payne D, Ahmad N (1969) The effect of the concentration and movement of solutions on the swelling, dispersion and movement of clay in saline and alkali soils. *Soil Sci* 27:129–139
- Serra J (1982) *Image analysis and mathematical morphology*. Academic Press, London
- Shainberg I, Letey J (1984) Response of soils to sodic and saline conditions. *Hilgardia* 52:1–57
- Shainberg I, Rhoades JD, Prather RJ (1981a) Effect of low electrolyte concentration on clay dispersion and hydraulic conductivity of a sodic soil. *Soil Sci Soc Am J* 45:273–277
- Shainberg I, Rhoades JD, Suarez DL, Prather RJ (1981b) Effect of mineral weathering on clay dispersion and hydraulic conductivity of sodic soils. *Soil Sci Soc Am J* 45:287–291
- Shainberg I, Levy GJ, Rengasamy P, Frenkel H (1992) Aggregate stability and seal formation as affected by drops' impact energy and soil amendments. *Soil Sci* 154:113–119

- Shainberg I, Levy GJ, Goldstein D, Mamedov AI, Letey J (2001) Prewetting rate and sodicity effects on the hydraulic conductivity of soils. *Aust J Soil Res* 39:1279–1291
- Šimunek J, van Genuchten MTh, Gribb MM, Hopmans JW (1998) Parameter estimation of unsaturated soil hydraulic properties from transient flow processes. *Soil Tillage Res* 47:27–36
- Soil Survey Staff (2010) Keys to soil taxonomy, 11th edn. USDA-Natural Resources Conservation Service, Washington, DC, p 338
- Somani LL (1991) Crop production with saline water. Agro Botanical Publishers, India
- Tamari S, Bruckler L, Halbertsma J, Chadoeuf J (1993) A simple method for determining soil hydraulic properties in the laboratory. *Soil Sci Soc Am J* 57:642–651
- Tedeschi A, Dell'Aquila R (2005) Effects of irrigation with saline waters, at different concentrations, on soil physical and chemical characteristics. *Agric Water Manag* 77:308–322
- Tedeschi A, Mele G, Terribile F (2002) Soil pore geometry changes in surface horizons under different irrigation regimes. In: Transactions of 17th World congress of soil science, 14–21 August 2002, Bangkok, Thailand
- Tedeschi A, Menenti M, Tedeschi P, Wang T, Xue X, Basile A, Mele G, De Lorenzi F, De Mascellis R, Di Matteo B, d'Andria R, Giorio G, Lavini A, Sorrentino G (2007) Design and evaluation of saline irrigation schedules to cope with droughts and scarce fresh water. In Topics 1: impacts of extreme hydrological events on irrigation and drainage of the ICID 22nd European regional conference, 2–7 September 2007, Pavia, Italy. http://www.italicid.it/Abstracts%20works/Proceedings_new.htm
- Van Genuchten MTh (1980) A closed-form equation for predicting the hydraulic conductivity of unsaturated soils. *Soil Sci Soc Am J* 44:892–898
- Varallyay G (1981) Extreme moisture regime as the main limiting factor of soil fertility of salt affected soils. *Agrokém Talajt* 30:73–96
- Varallyay G, Szabolcs I (1974) Special water problems in salt affected soils. In: Transactions of 10th international symposiums on Agrochimica. Water in Agriculture. Bari, 1974. *Agrochimica* 18 277–287
- Vervoort RW, Cattle SR (2003) Linking hydraulic conductivity and tortuosity parameters to pore space geometry and pore size distribution. *J Hydrol* 272:36–49
- Vogel HJ, Roth K (1998) A new approach for determining effective soil hydraulic functions. *Eur J Soil Sci* 49:547–556
- Vogel HJ, Roth K (2001) Quantitative morphology and network representation of soil pore structure. *Adv Water Resour* 24:233–242
- Wang Y, Li Y, Xiao D (2008) Catchment scale spatial variability of soil salt content in agricultural oasis, Northwest China. *Environ Geol* 56:439–446
- Wooding RA (1968) Steady infiltration from a shallow circular pond. *Water Resour Res* 4:1259–1273